4-2015

HETEROGENEITY OF INFILTRATION RATES IN ALLUVIAL FLOODPLAINS AS MEASURED WITH A BERM INFILTRATION TECHNIQUE

Derek M. Heeren
University of Nebraska-Lincoln, derek.heeren@unl.edu

Garey A. Fox
Oklahoma State University, gafox2@ncsu.edu

Daniel E. Storm
Oklahoma State University

HETEROGENEITY OF INFILTRATION RATES IN ALLUVIAL FLOODPLAINS AS MEASURED WITH A BERM INFILTRATION TECHNIQUE

D. M. Heeren, G. A. Fox, D. E. Storm

ABSTRACT. *Hydrologic heterogeneities (e.g., macropores and gravel outcrops) in floodplains are hypothesized to play an integral role in impacting flow and leaching between the soil surface and shallow alluvial aquifers, which are intricately connected to streams. Infiltration is often assumed to be uniform, but this neglects the spatial variability common in anisotropic, heterogeneous alluvial floodplain soils. The objective of this research was to quantify infiltration and hydraulic conductivity across a range of scales (point to 100 m^2) using a berm infiltration technique. Plot-scale leaching experiments were performed across a range of soil types at each of three floodplain sites in northeastern Oklahoma and northwestern Arkansas. Plots maintained a constant head of 2 to 9 cm for up to 52 h. Effective saturated hydraulic conductivity (K_{eff}), based on plot-scale infiltration rates and a one-dimensional Darcy flow equation, ranged between 0.6 and 68 cm h^{-1} and varied considerably even within a single floodplain. The K_{eff} was also calculated at the point scale using particle size distributions and Retention Curve (RETC). Point-scale estimates were significantly lower than plot-scale K_{eff} and also failed to capture the variability of K_{eff}. The estimated permeability of the limiting layer reported in soil surveys was consistent with point-scale estimates of K_{eff} but was lower than plot-scale K_{eff} at most sites. Tension infiltrometers showed that macropores accounted for approximately 84% to 99% of the total saturated hydraulic conductivity. The plot scale (1 to 100 m^2) generally appears to be within the representative elementary volume (REV), but drift in K_{eff} occurs beyond the REV due to changing geomorphic formations. Plot-scale infiltration tests are recommended over point-scale estimates, although only small plots (1 m × 1 m) are necessary.*

Keywords. *Gravel outcrop, Infiltration, Ozark ecoregion, Plot scale, Preferential flow, Representative elementary volume.*

Due to their characteristics such as geomorphic depositions, their abundant roots and other biological activity, and frequent drying/wetting cycles, alluvial floodplains and their riparian areas are particularly susceptible to preferential flow (Mulholland et al., 1990; Gold and Kellogg, 1997; Carlyle and Hill, 2001; Vellidis et al., 2001; Polyakov et al., 2005; Fuchs et al., 2009). Linear deposits of coarse-grained sediments with high infiltration rates such as gravel outcrops and macropores create preferential flow paths (Gotovac et al., 2009; Najm et al., 2010). These flow paths can link distant floodplains areas directly to streams.

Infiltration is often assumed to be uniform at the field scale, but this neglects the high spatial variability (Biggar and Nielsen, 1976; Vieira et al., 1981) common in anisotropic, heterogeneous alluvial floodplain soils (Heeren et al., 2010, 2011, 2014b). For water movement through soil, macropores have been shown to have a large impact on flow and solute transport (Thomas and Phillips, 1979; Fox et al., 2004; Djodjic et al., 2004; Akay and Fox, 2007; Gotovac et al., 2009). Gold and Kellogg (1997) specifically called for the development of unique sampling schemes and simulation models for situations where substantial infiltration occurs through preferential flow pathways, but limited work in monitoring, theoretical model development, and application has been achieved to date.

While surface runoff is considered to be the primary transport mechanism for nutrients such as phosphorus (Gburek et al., 2005), subsurface transport through coarse subsoil to gravel bed streams may be significant and represents a source of P not alleviated by current conservation practices (e.g., riparian buffers). However, relatively few studies on infiltration and P leaching have been done at the plot scale where infiltration and transport may be controlled by heterogeneity present at various scales (Nelson et al., 2005). Vellidis et al. (2001) specifically noted that preferential flow paths allowed nutrient plumes to bypass a riparian buffer.

Accounting for spatial variability in infiltration rates is important not only for watershed flow and nutrient

Submitted for review in November 2014 as manuscript number NRES 11056; approved for publication by the Natural Resources & Environmental Systems Community of ASABE in April 2015. Presented at the 2013 ASABE Annual Meeting as Paper No. 131621213.

The authors are **Derek M. Heeren, ASABE Member,** Assistant Professor, Department of Biological Systems Engineering, University of Nebraska-Lincoln, Nebraska; **Garey A. Fox, ASABE Member,** Professor and Orville L. and Helen L. Buchanan Chair, Department of Biosystems and Agricultural Engineering, and Director and Thomas E. Berry Endowed Professor in Water Research and Management, Oklahoma Water Resources Center, Oklahoma State University, Stillwater, Oklahoma; **Daniel E. Storm, ASABE Member,** Professor, Department of Biosystems and Agricultural Engineering, Oklahoma State University, Stillwater, Oklahoma. **Corresponding author:** Derek Heeren, 241 L.W. Chase Hall, University of Nebraska-Lincoln, Lincoln, NE 68583-0726; phone: 402-472-8577; e-mail: derek.heeren@unl.edu.

  ISSN 2151-0032 DOI 10.13031/trans.58.11056

transport models but also for management of variable-rate irrigation (Evans et al., 2012), which can account for in-field heterogeneity in soil properties. Easton (2013) used geostatistics to study spatial trends in infiltration rate on a hillslope and found that "methods of measuring the infiltration rate of a soil differ in first-order statistical measures (mean and variance), but not substantially in second-order statistical measures (spatial structure)."

As the scale of measurement increases, the physical properties of a porous medium like soil tend to have decreasing variability until a representative elementary volume (REV) is reached (Bear, 1972; Brown et al., 2000). The REV is bounded by a minimum (V_{min}) and maximum (V_{max}) volume. For measurement volumes less than V_{min}, the property fluctuates rapidly in space due to the influence of individual pores. For measurement volumes above V_{max}, "additional morphological structures allow the property to drift to new values, which results in large field variability" (Brown et al., 2000). While the REV was originally applied to small scales, the influence of infrequent but large macropores, especially on hydraulic conductivity, may justify applying the REV to larger scales. Beven and Germann (1981, 1982) suggest an REV for macropore porosity that would occur at a length scale of two to three orders of magnitude higher than an REV for the micropore porosity. Increasing the diameter of double ring infiltrometers has been found to reduce the variability of measured infiltration rates (Sisson and Wierenga, 1981; Lai and Ren (2007). However, whether double ring infiltration can be scaled up to the plot or field scale has not been well established. Easton (2013) found that using the sprinkler frame infiltration method with a measurement area of 20 m^2 resulted in lower mean infiltration rates and lower variation in infiltration rates compared to using a ponded double ring infiltrometer (23 cm diameter) or sprinkler ring infiltrometer (24 cm diameter). Massman (2003) observed that hydraulic conductivities measured with flood tests in infiltration basins were up to two orders of magnitude higher or lower than hydraulic conductivities determined from air conductivity or calculated from grain size parameters.

In this research, it was hypothesized that as the scale of measurement increases, the measured infiltration rate and hydraulic conductivity of the topsoil will increase due to large but infrequent macropores, and that the variability will decrease, until an REV is attained. Therefore, the objective was to quantify infiltration and effective hydraulic conductivity across a range of scales (point to 100 m^2) to evaluate the potential for heterogeneous infiltration in alluvial floodplains. Accurately understanding infiltration is essential for understanding nutrient and contaminant transport.

Materials and Methods

Alluvial Floodplain Sites

The alluvial floodplain sites were located in the Ozark ecoregion of northeastern Oklahoma and northwestern Arkansas (fig. 1). The Ozark ecoregion of Missouri, Arkansas, and Oklahoma is approximately 62,000 km^2 and is characterized by gravel bed streams and cherty soils in the riparian floodplains. The erosion of carbonate bedrock (primarily limestone) by slightly acidic water has left a large residuum of chert gravel in Ozark soils, with floodplains generally consisting of coarse chert gravel overlain by a mantle (1 to 300 cm) of gravelly loam or silt loam. The alluvium is spatially heterogeneous, resulting in preferential flow pathways that are hypothesized to be ancient buried gravel bars (Heeren et al., 2010). Similar hydrogeologic conditions exist near gravel bed streams in their associated alluvial floodplains worldwide.

Figure 1. Selected alluvial floodplain sites for plot-scale infiltration experiments in the Ozark ecoregion (adapted from Heeren et al., 2014a).

Vertical electrical resistivity profiles were collected at the floodplain sites to characterize the heterogeneity of the unconsolidated floodplain sediments (Miller, 2012; Miller et al., 2014). Electrical resistivity imaging (ERI) data were collected using a SuperSting R8/IP Earth resistivity meter (Advanced GeoSciences, Inc., Austin, Tex.) with 56-electrode arrays. The profiles typically employed electrode spacings of 1 to 1.5 m with an associated depth of investigation of approximately 13 m, which included the vadose zone, alluvial aquifer, and bedrock. The resistivity sampling with the SuperSting R8/IP and subsequent inversion used a proprietary routine devised by Halihan et al. (2005), which produced higher-resolution images than conventional techniques.

The Barren Fork Creek site (fig. 2; 35.90° N, 94.85° W) is immediately downstream of the Eldon Bridge gauge station (USGS 07197000). With a watershed size of 845 km^2, Barren Fork Creek is a fourth-order stream with a historical median discharge of 3.6 $m^3\ s^{-1}$. The study area at Barren Fork Creek was located on the outside of a meander bend that was being actively eroded by the stream (Midgley et al., 2012). The soils were classified as Razort gravelly loam underlain with alluvial gravel deposits. Thickness of the loam ranged from 0.3 to 2.0 m, with dry bulk densities ranging from 1.3 to 1.7 g cm^{-3}. Soil hydraulic studies on these soil types have shown that subtle morphological features can lead to considerable differences in soil water flow rates (Sauer and Logsdon, 2002; Sauer et al., 2005).

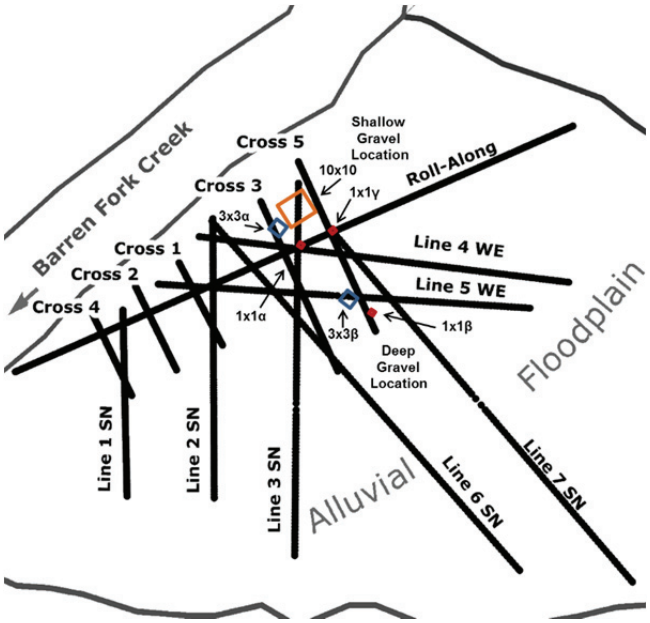

Figure 2. Barren Fork Creek floodplain site, including locations of plots for infiltration experiments (labeled according to plot size in m). Thick black lines are locations of electrical resistivity profiles (Miller, 2012, appendix A; Miller et al., 2014), which were used to select plot locations. For orientation, north is up. The floodplain is bounded by Barren Fork Creek to the northwest, a small tributary to the northeast, and a bluff to the south.

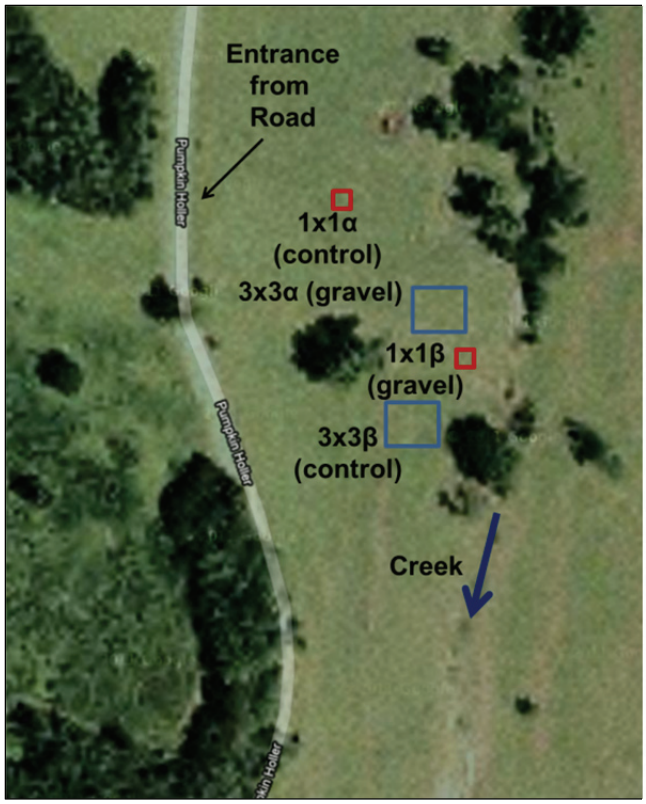

Figure 3. Pumpkin Hollow floodplain site, including locations of plots for infiltration experiments (labeled according to plot size in m). For orientation, north is up. The floodplain is bounded by Pumpkin Hollow Creek to the east and a bluff to the west. Background electrical resistivity profiles (not shown) were located just south of the plot locations.

The Pumpkin Hollow floodplain site (fig. 3) was also located in the Ozark ecoregion of northeastern Oklahoma (36.02° N, 94.81° W). A small tributary of the Illinois River, Pumpkin Hollow Creek is a first-order ephemeral stream in its upper reaches. The entire floodplain was 120 to 130 m across at the research site, with an estimated watershed area of 15 km^2. The land use at the site was pasture for cattle. The Pumpkin Hollow field site was a combination of Razort gravelly loam and Elsah very gravelly loam, although infiltration experiments were limited to the Razort gravelly loam soils. Topsoil thickness ranged from 0 to 3 cm, and bulk densities of the cohesive material were between 1.3 to 1.5 g cm^{-3}.

The Clear Creek alluvial floodplain site (fig. 4) was located just west of Fayetteville, Arkansas, in the Arkansas River basin and flows into the Illinois River (36.13° N, 94.24° W). The total drainage area is 199 km^2 for the entire watershed. Land use in the basin was 36% pasture, 34% forest, 27% urban, and 3% other. Soils were loamy and silty, deep, moderately well drained to well drained (U.S. EPA, 2009) and generally contained less chert or gravel than the Barren Fork Creek or Pumpkin Hollow floodplain sites. Thickness of the top loam layer ranged from 0.3 to 2.0 m, with dry bulk densities ranging from 1.5 to 1.7 g cm^{-3}. Clear Creek is a fourth-order stream with a flow of approximately 0.5 m^3 s^{-1} at the study site, and the area of the watershed above that point was 101 km^2. The land use in the study area was pasture and consisted of Razort gravelly loam soils.

Plot-Scale Infiltration and Hydraulic Conductivity

Measuring infiltration rates and/or leaching of solutes at plot scale is difficult, especially for high hydraulic conductivity soils, without innovative field methods. In this research, the berm method (Heeren et al., 2014a) was used to confine infiltration plots and maintain a constant head of water, with plot sizes ranging from 1 m × 1 m to 10 m × 10 m (fig. 5). The berm method consists of four sections of 15 cm diameter vinyl hose that were attached to 90° steel elbows and surrounded the infiltration gallery. Each elbow had an air vent, and one elbow had a gate valve with a garden hose fitting for water. The vinyl hoses were secured to the elbows with stainless steel hose clamps and sealed with silicone sealant. The berms were then partially filled with water to add weight, but excess pressure was avoided to ensure the vinyl hoses did not separate from the elbows. A shallow trench (3 to 5 cm) was cut through the thatch layer and a thick bead of liquid bentonite was used to create a seal between the berm and the soil. High-density polyethylene tanks (4.9 and 0.76 m^3) were used to mix the stream water and solutes used in simultaneous infiltration and leaching experiments (the leaching aspects of the project are not discussed in this article). A combination of 5.1 cm diameter PVC with manual valves and garden hoses with float valves were used to deliver water (gravity fed) from the tanks to the plots. When a tank was nearly empty, flow was temporarily stopped while the tank was refilled and solutes were added and mixed. The largest plot sizes (10 m × 10 m) required continuous pumping and solute injection

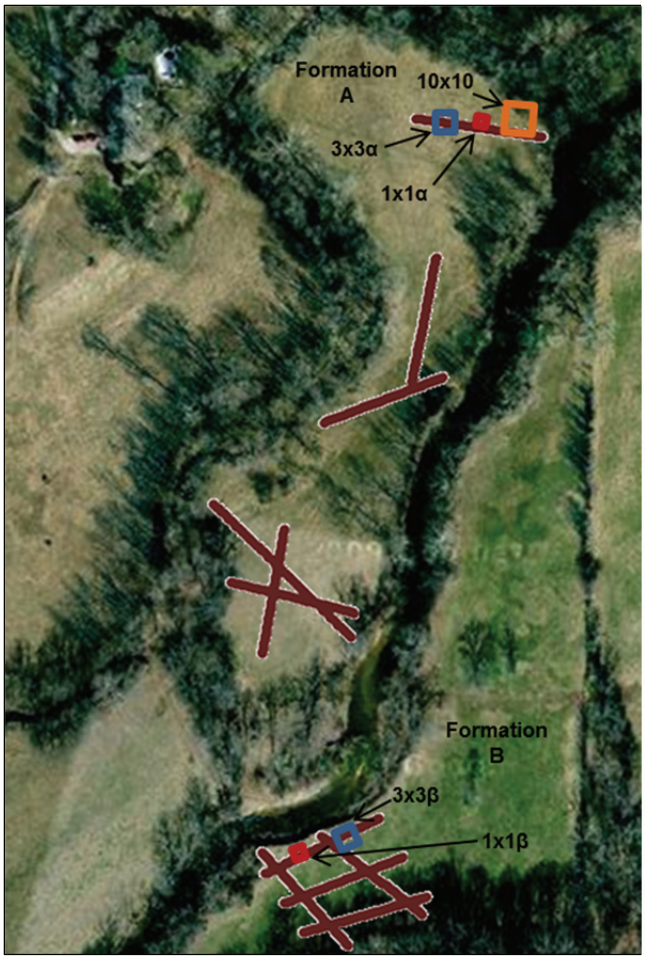

Figure 4. Clear Creek floodplain site, including locations of plots for infiltration experiments (labeled according to plot size in m). Thick maroon lines are locations of electrical resistivity profiles (Heeren, 2012, appendix A), which were used to select plot locations. For orientation, north is up. Within the floodplain, Formation A is bounded by Clear Creek to the east and a small overflow channel to the north and west, and Formation B is bounded by Clear Creek to the north and a bluff to the south.

directly into the pump hose using Dosatron injectors (D8R, Dosatron, Clearwater, Fla.) instead of using tanks for mixing. Constant heads in the plots were maintained (Heeren et al., 2014a) between 3 and 10 cm. Depth to the water table ranged from 50 cm at the Pumpkin Hollow site to 350 cm at the Clear Creek site.

Four to six infiltration experiments were performed at each site with plots selected to represent a range of infiltration rates at each floodplain site (figs. 2 to 4, table 1). Plots were located on relatively level areas in order to minimize the variation in water depth across the plot. Larger plots were required to have smaller slopes to ensure that the entire plot could be inundated without overflowing the berm.

A brief survey of the literature was performed to determine the best method to determine effective saturated hydraulic conductivity (K_{eff}) from plot-scale constant-head infiltration rate data. Transient solutions are available for early time infiltration data (e.g., Philip, 1957; eq. 1) for one-dimensional infiltration. A quadratic equation can be fit to the data in order to determine two parameters: K_{eff} and sorptivity, the latter of which accounts for both capillary action and depth of the water above the soil surface (head). For the long-duration (3 to 52 h) plot-scale experiments, the depth of infiltration often exceeded the top layer of soil, violating the homogeneous assumption in these equations. It was also difficult to get precise transient early time data when accounting for measurement error and the change in storage of water above the soil surface during plot-scale experiments.

The second major category of equations for predicting K_{eff} from infiltration data is steady-state equations (Bodhinayake et al., 2004). Most of the plots were run long enough to achieve quasi-steady-state conditions, with total infiltration often greatly exceeding the depth of the top layer of soil. Without transient data, more parameters are needed for these solutions (ponded depth, geometry to account for two-dimensional (radial) effects, etc.). However, a good solution for our situation, with two distinct soil layers, was not found.

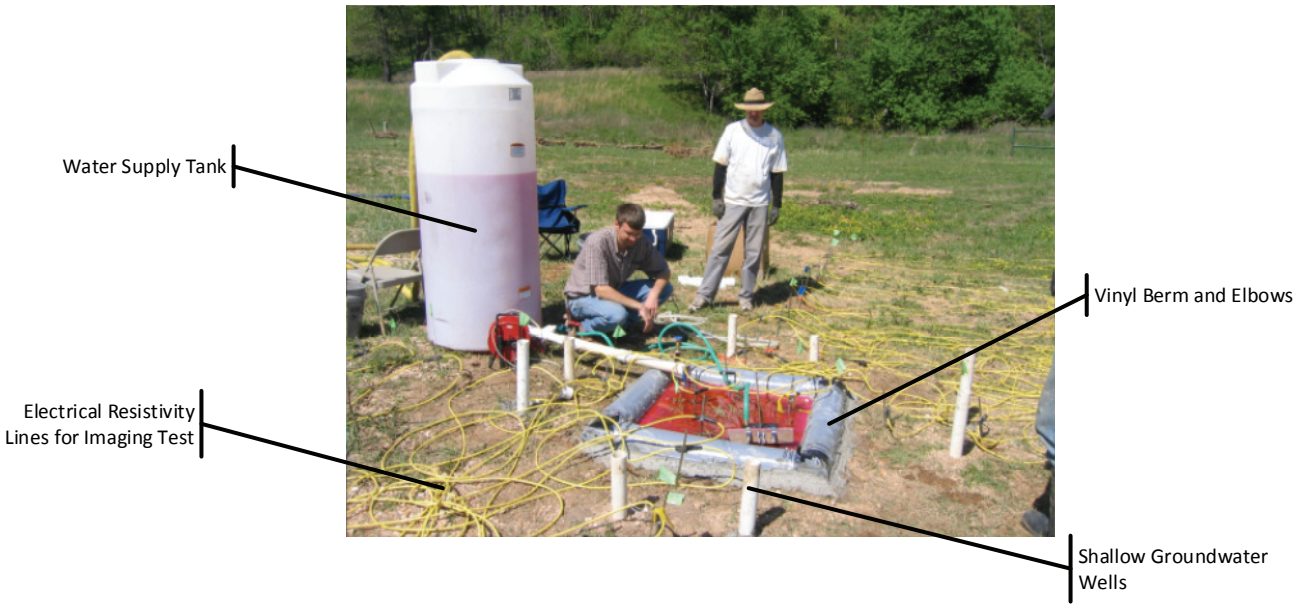

Figure 5. Field installation of the berm infiltration method.

Table 1. Infiltration experiments at three alluvial floodplain sites in the Ozark ecoregion.

Floodplain Site	Date (m/d/y)	Plot[a]	Area (m^2)	Treatment	Duration (h)	Steady-State Infiltration (q, cm h^{-1})	Limiting Layer Depth (d, cm)	Average Head (h, cm)	Hydraulic Gradient (i, cm cm^{-1})	Hydraulic Conductivity (K_{eff}, cm h^{-1})
Barren Fork	6/30/11	1×1 α	1	Shallow gravel	22	10	92	5.8	1.06	9.6
	6/30/11	3×3 α	9	Shallow gravel	22	13	110	3.1	1.03	12
	7/13/11	1×1 β	1	Deep gravel	46	6.8	134	4.7	1.04	6.6
	7/13/11	3×3 β	9	Deep gravel	48	3.0	145	6.4	1.04	2.9
	5/7/12	10×10	60[b]	Shallow gravel	4	13	107	3.0	1.03	13
	6/6/12	1×1 γ	1	Shallow gravel	86	14	113	9.0	1.08	13
Pumpkin Hollow	5/4/11	1×1 α	1	Control	32	5.3	99	6.8	1.07	5.0
	5/5/11	3×3 α	9	Gravel outcrop	2.8	18	46	5.4	1.12	16
	6/1/11	1×1 β	1	Gravel outcrop	4.3	74	36	3.2	1.09	68
	6/2/11	3×3 β	9	Control	24	6.3	58	6.5	1.11	5.7
Clear Creek	4/12/11	1×1 α	1	Formation A	41	5.6	57	1.8	1.03	5.4
	4/12/11	3×3 α	9	Formation A	41	3.3	76	1.8	1.02	3.2
	7/27/11	1×1 β	1	Formation B	48	1.3	137	6.3	1.05	1.2
	7/27/11	3×3 β	9	Formation B	45	0.8	210	7.2	1.03	0.7
	5/21/12	10×10	100	Formation A	52	0.6	84	6.0	1.07	0.6

[a] α, β, and γ indicate the first, second, and third set of infiltration experiments performed at a field set.
[b] Pump capacity was not sufficient to keep the entire infiltration gallery inundated.

Therefore, Darcy's law was applied specifically to the top layer of soil for steady-state infiltration under a constant head. Since edge effects were considered small compared to the large area of the infiltration gallery at the plot scale, one-dimensional vertical flow was assumed at the plot scale. Equation 1 is for infiltration into a lower conductivity layer underlain by a higher conductivity layer:

$$q = K_{eff} i = K_{eff}\left(1 + \frac{h}{d}\right) \quad (1)$$

where q is the steady-state infiltration rate (L T^{-1}), K_{eff} is the effective field saturated hydraulic conductivity (L T^{-1}), i is the hydraulic gradient (L L^{-1}), h is the spatially and temporally averaged depth of water in the infiltration gallery (L), and d is the depth of the top layer of soil. The first term in the parentheses represents the hydraulic gradient due to gravity, which is a unit gradient. The second term is the gradient due to the change in pressure head over the length of flow. Water pressure at the soil surface is the hydrostatic pressure head associated with the spatially and temporally averaged depth of water in the plot. As water flows from a restrictive layer of soil into a more conductive layer, an inverted water table will form. It was assumed that the inverted water table would occur approximately at the bottom of the restrictive layer, indicating a pressure head of zero at the bottom of the top layer of soil. It is acknowledged that the one-dimensional flow assumption is a limitation of this approach when considering the heterogeneity and anisotropy of these complex alluvial deposits (Fox et al., 2011).

For 1 m × 1 m and 3 m × 3 m plots, q was determined based on flow rates from the tanks. The tanks were instrumented with automated water level data loggers with an accuracy of 0.5 cm (HoboWare U20, Onset Computer Corp., Bourne, Mass.) to monitor water depth (pressure) and temperature at 1 min intervals. An additional water level data logger was used to monitor the atmospheric pressure. Logger data were processed with HoboWare Pro software, which adjusted for changes in atmospheric pressure and water density. Measured tank water depth over time was used to calculate the flow rate using a volumetric rating curve. For the 10 m × 10 m plots, flow was measured based on the frequency of cycles in the Dosatron injectors (D8R, Dosatron, Clearwater, Fla.). The h was determined from automated water level data loggers (HoboWare U20, Onset Computer Corp.) placed in the plots along with manual measurements of water depth.

The d of the silt loam layer was determined from soil cores within and near the plots. The Barren Fork Creek site had a distinct layer change from silt loam to coarse gravel. The Pumpkin Hollow site was highly heterogeneous, and it was sometimes difficult to identify the bottom of a restrictive layer. In some cases (e.g., gravel outcrops), the majority of the flow would have been lateral flow above a restrictive layer. Field observations indicated that the matrix of the limiting layer in some plots may not have been completely saturated at the conclusion of the infiltration experiment. With these limitations in mind, the results were termed effective saturated hydraulic conductivity (K_{eff}). While not precise, this method allowed us to compare values for a soil property that varies across orders of magnitude.

Point-Scale Hydraulic Conductivity

During the installation of the observation wells with a Geoprobe 6200 TMP (trailer-mounted probe) direct-push drilling machine (Geoprobe Systems, Salina, Kans.), which has been shown to be effective in coarse gravel aquifers (Miller et al., 2011), soil core samples were collected at known depths using a dual-tube core sampler with a 4.45 cm opening. The sampler opening size limited the particle size that could be sampled, and large cobbles occasionally clogged the sampler, resulting in incomplete cores for that depth interval. Geoprobe soil coring typically began at the soil surface and proceeded to or past the water table (0.5 to 3.5 m below ground surface). Cores were recovered from one to four wells per plot.

A subset of the soil core samples were dry sieved with a sieve stack ranging from 2.0 to 12.5 mm for a particle size analysis. Sample preparation included disaggregation with

a rubber-tipped pestle when necessary. If particles were retained on the 12.5 mm sieve, a measurement of the *b* axis (longest intermediate axis perpendicular to the long *a* axis) of the largest particle was used as the sieve size that 100% of the sample would pass through because that dimension largely controls whether a particle will pass a particular sieve (Bunte and Abt, 2001).

A complete textural analysis was desired for surface soil samples from one soil core per plot. Following the procedure developed by Miller et al. (2014), the particle size distribution (PSD) of the mass passing the finest sieve (2 mm) "was determined using a Cilas 1180 particle size analyzer (Cilas USA, Madison, Wisc.), which calculated the ratio of particle sizes based on the obscurance of a laser beam. The Cilas 1180 measured the relative volume for particle size ranges of a representative sample. The PSD of the fine fraction was calculated by multiplying the percent distribution from the sample by the total volume of the fine dry-sieved fraction."

Point-scale K_{eff} was calculated based on a topsoil sample from one soil core per plot, as described above. Using the PSD determined by sieving and the Cilas particle size analyzer, K_{eff} was calculated by Retention Curve (RETC) with the van Genuchten equation using the Mualem assumption (van Genuchten et al., 1991). RETC requires the percent sand, silt, and clay according to the USDA soil classification, which defines clay as particles smaller than 2 μm. Since the Cilas particle size analyzer only measured down to 3.9 μm, a minor amount of extrapolation was required to extend the PSD to 2 μm. In order to best account for this source of uncertainty, both a low and high clay content were estimated for each sample. RETC was used for both clay contents, and the average of the two K_{eff} values was taken to be the K_{eff} for that sample. Since RETC only used sand, silt, and clay percentages, one of the limitations of this method is that it does not account for the gravel content.

TENSION INFILTROMETERS AND MATRIX HYDRAULIC CONDUCTIVITY

After the plot infiltration experiments, mini-disk infiltrometers (Decagon Devices, Pullman, Wash.) were used inside the plots (after the soil profile had dried) to measure soil matrix hydraulic conductivity. The tension infiltrometers measured unsaturated soil infiltration rates by using a 4.5 cm steel disk to expose water that is under tension (negative pressure) to the soil surface. Water must flow from a higher potential to a lower potential. Therefore, water under tension infiltrated into the soil matrix, which had a more negative capillary pressure. However, the water did not infiltrate into the macropores, which had a less negative capillary pressure. Since the macropores remained dry, flow was restricted to the soil matrix, with the infiltration rate equivalent to matrix infiltration.

Suction levels of 1, 3, and 6 cm, spanning the ability of the infiltrometer, were used. Equivalent radii were calculated for each suction level with the capillary rise equation (Scott, 2000):

$$h = \frac{2\sigma\cos\theta}{r\rho_w g} = \frac{0.15}{r} \quad (2)$$

where h is the capillary rise or suction (L), σ is the surface tension of water (F L^{-1}), θ is the contact angle, r is the equivalent radius (L), ρ_w is the density of water (M L^{-3}), and g is the acceleration due to gravity (L T^{-2}). The value of θ was assumed to be zero, and σ was assumed to be 72.8 mN m^{-1} (for water at 20°C). The unit conversion coefficient of 0.15 arises for h and r in cm.

In order to enable the comparison between suction level and pore geometry, the following conceptual model was used. The soil pore space was conceptualized as circular tubes (not necessarily vertical) with a distribution of radii. Each pore was considered either activated (saturated) or dry. For a given suction level, the infiltration is limited to pores with radii less than or equal to the radius corresponding to the suction level. A comparison between plot infiltration data (all pores activated) and tension infiltrometer was used to differentiate between matrix and macropore flow. The simplification in this conceptualization is that it neglects flow in a thin film along a pore wall when that pore is unsaturated. Accounting for thin film flow in macropores would increase their contribution; therefore, this approach gives a conservative estimate of the impact of macropores.

Soils pores have been classified as macropores (greater than 75 μm), mesopores (30 to 75 μm), and micropores (5 to 30 μm) (SSSA, 2008). In this research, macropores were defined as pore spaces with equivalent diameters of 500 μm (correlating to 6 cm capillary pressure) or more due to limitations of the infiltrometer. The unsaturated hydraulic conductivity was calculated from the tension infiltrometer results using a transient solution (Zhang, 1997). Readings were taken until the infiltrometer reservoir was depleted (14 to 121 min), which was sufficient to fit the hydraulic conductivity and sorptivity to the cumulative infiltration versus time data.

For a fully saturated soil profile, hydraulic equilibrium exists between the matrix and macropores, which then have identical vertical hydraulic gradients. The total flow (infiltration) is a function of the total saturated hydraulic conductivity (K_s, L T^{-1}), which, for these conditions, is simply a composite of the hydraulic conductivity in each domain (following Simunek et al., 2003):

$$K_s = K_{s,mx} + K_{s,mp} \quad (3)$$

where $K_{s,mx}$ (L T^{-1}) is the saturated hydraulic conductivity of the matrix, and $K_{s,mp}$ (L T^{-1}) is the saturated hydraulic conductivity of the macropore domain. The $K_{s,mx}$ was equal to the hydraulic conductivity calculated from the tension infiltrometer data with a 6 cm capillary pressure, and the K_s was approximated with K_{eff} calculated from the infiltration plots. Equation 3 was used to determine $K_{s,mp}$ in order to determine the significance of macropore flow compared to total infiltration.

RESULTS AND DISCUSSION

PLOT AND POINT SCALE INFILTRATION AND HYDRAULIC CONDUCTIVITY

Calculated K_{eff} using equation 1 for the plot-scale experiments varied widely across sites and within sites, ranging from 0.5 to 68 cm h^{-1} (table 1). Infiltration plots at the Barren Fork Creek site were located in two areas based on ERI data (Miller, 2012; Miller et al., 2014): where the gravel formation was under a thick mantle of silt loam ("deep gravel"), and on a buried gravel bar where the gravel was closer to the current ground surface ("shallow gravel"). During the plot-scale infiltration experiments, hydraulic gradients ranged from 1.03 to 1.08 cm cm^{-1} (fig. 2, table 1). Infiltration rates ranged from 3.0 to 6.8 cm h^{-1} for the deep gravel plots and from 10 to 14 cm h^{-1} for the plots with shallow gravel. The calculated K_{eff} values were similar, ranging from 2.9 to 6.6 cm h^{-1} for the deep gravel plots and from 9.6 to 13 cm h^{-1} for the shallow gravel plots. The expected pattern of higher K_{eff} in the shallow gravel location compared to the deep gravel location held for plot-scale data.

In order to analyze spatial variability in the soil properties at the Barren Fork Creek site, geostatistics were performed on the electrical resistivity data (Miller, 2012), which have been correlated to hydraulic conductivity (Miller et al., 2014). The geostatistical program GS+ (Gamma Design Software, LLC, Plainwell, Mich.) was used to analyze the top layer (approximately 0.0 to 0.2 m below ground surface) and the second layer (approximately 0.2 to 0.5 m below ground surface) of log-transformed electrical resistivity (Ω-m). While the top layer would be closer to where the infiltration occurs, the second layer of electrical resistivity was more reliable and was usually still be within the silt loam at the Barren Fork site. Both isotropic and anisotropic variograms were created, although the anisotropic variograms did not reveal strong directional patterns in either layer. This is in contrast to previous research that found strong directional patterns in the deeper gravel subsoil (Miller, 2012), likely related to ancient gravel bars and abandoned stream channels. Results from the exponential isotropic model (fig. 6) showed greater variability in the top layer but a similar pattern for both layers. The range (A_0), beyond which data were not autocorrelated, was 27 m and 20 m for the top and second layers, respectively. These A_0 data may indicate the approximate scale of the V_{max}, where the REV ends and K_{eff} begins to drift due to changing geomorphic formations. The A_0 from the Barren Fork Creek site were comparable to Easton (2013), who reported A_0 from 17 m to 34 m for infiltration rates on an Arkport fine sandy loam soil hillslope (11% average slope). An interesting comparison, though, is that Easton (2013) found the nugget to be zero in most cases for infiltration rate, where the Barren Fork Creek site had a non-zero nugget for electrical resistivity.

Plots at the Pumpkin Hollow field site were located in gravel outcrops and control locations (fig. 3). Gravel outcrops in the floodplain appeared to be gravel splays from a recent high-flow event (on the order of a 50-year recurrence interval) rather than an exposed buried gravel bar. A

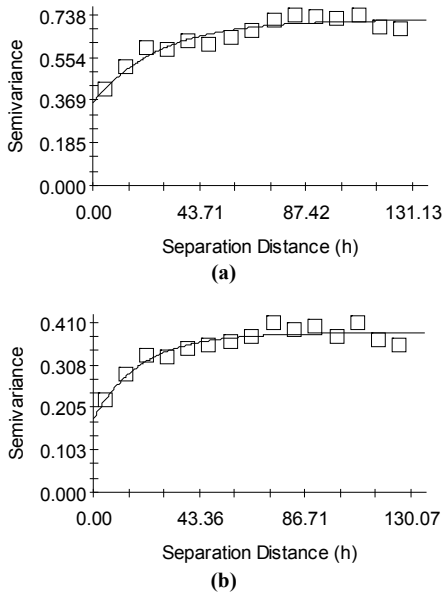

Figure 6. Variograms for the Barren Fork Creek site based on the (a) top layer (approximately 0.0 to 0.2 m below ground surface) and (b) second layer (approximately 0.2 to 0.5 m below ground surface) of log-transformed electrical resistivity data. The *x*-axis is separation distance, *h* (m).

10 m × 10 m plot was not performed at the Pumpkin Hollow site due to insufficient water supply in the small ephemeral creek. During the plot-scale infiltration experiments, measured hydraulic gradients ranged from 1.07 to 1.12 cm cm^{-1} with calculated K_{eff} from equation 1 ranging from 5.0 to 5.7 cm h^{-1} for the control plots and from 16 to 68 cm h^{-1} for the gravel outcrop plots (table 1). This wide range indicates considerable heterogeneity in infiltration processes at the Pumpkin Hollow floodplain due to the occurrence of gravel outcrops. This range is remarkable considering the close proximity of the plots. For example, the 1×1 β and 3×3 β plots (fig. 3) were approximately 10 m apart and had K_{eff} values of 68 and 5.7 cm h^{-1}, respectively. The very high conductivity gravel outcrops achieved quasi-steady-state flow quickly, resulting in relatively short (less than 5 h) plot infiltration experiments. Results from the Pumpkin Hollow site were dominated by spatial variability in soils, indicating that distance between plots may have been larger than the V_{max} where the REV ends. Rapid water movement might be occurring not only vertically in these soils but also laterally through zones of coarser soils and gravels, as suggested by Fox et al. (2011), who conducted flow and injection experiments over a 2 to 3 m scale. For the 3 m × 3 m gravel outcrop plot at the Pumpkin Hollow site, which had a steady-state infiltration rate of 18 cm h^{-1}, infiltrating water flowed through a preferential flow path approximately 15 m to the stream in less than 3 h (fig. 7).

Infiltration plots at the Clear Creek floodplain site were located in two unique geomorphic formations (fig. 4). Formation A, located on the west side of the creek, was very similar to the alluvial deposits at the Barren Fork Creek site, with an apparently uniform layer of silt loam (0.5 to 1.0 m) above chert gravel that generally extended downward to limestone bedrock. Unlike the Barren Fork Creek

Figure 7. Infiltrating water from the 3 m × 3 m gravel outcrop plot at the Pumpkin Hollow site flowed through a preferential flow path to the stream, as shown by Rhodamine WT dye.

site, the gravel in Formation A contained a buried soil horizon with potential for a perched water table. Formation B, located on the east side of the creek, was very gravelly at the surface but the gravel had a high enough proportion of fines to cause low infiltration rates. The streambank profile at Formation B was 3.5 m tall, with a very thick limiting layer (silt loam) ranging from 2.1 to 2.4 m deep (table 1). At this location, Clear Creek is a bedrock stream, with the

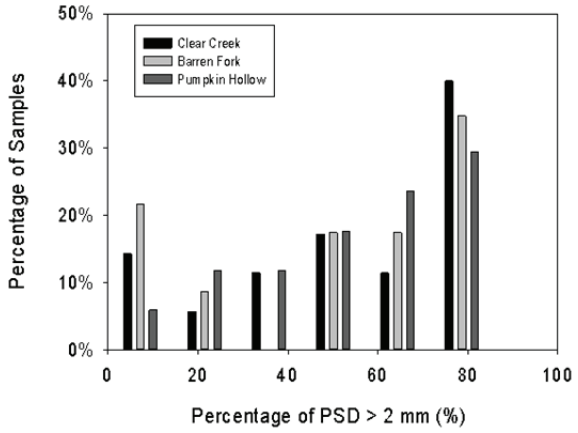

Figure 8. Particle size distributions (above 2 mm) of soil core samples using six bins for each histogram.

water table in the alluvial aquifer being essentially at bedrock (determined by auger refusal with the Geoprobe drilling machine) during baseflow conditions. Plot-scale infiltration rates were lower than at the other sites, ranging from 0.7 to 5.4 cm h^{-1} (table 1).

Particle size analysis of soil core samples also showed large heterogeneity in soils (fig. 8). Point-scale soil cores suggested that the soils were heterogeneous, even within a small area of a given floodplain (fig. 8). At the Barren Fork site, this was primarily due to vertical variation in the soil profile (silt loam underlain by gravel), while at the other sites the variability was more spatially dependent at the soil surface. The RETC-calculated K_{eff} ranged between 0.6 and 3.0 cm h^{-1} with limited variability (typically no more than 1.0 cm h^{-1}) at each site. It is not surprising that the plot-scale calculated K_{eff} is higher than the K_{eff} estimated using a pedotransfer function because of the presence of gravels within the alluvial floodplain soils. The pedotransfer function database was constructed primarily on soil samples from cultivated agricultural land. A unique aspect of this research was documenting the magnitude of the expected differences between the techniques for gravelly soils in alluvial floodplains.

Point versus Plot Scale Conductivity

Data from the plot-scale experiments were compared to point-scale estimates of K_{eff} and the estimated permeability of the limiting layer reported by the USDA Natural Resources Conservation Service (NRCS, 2012). The reported NRCS soil survey estimated K_{eff} ranged from 1.5 to 5 cm h^{-1} for the Razort gravelly loam soil present at all three sites (fig. 9). Five of the six plot-scale data at Barren Fork Creek were higher than the maximum predicted by the NRCS soil survey as well as the point-scale estimates. The Barren Fork Creek point-scale estimates did not capture the variability in K_{eff} shown in the plot-scale data, which may be partly due to the fact that point-scale estimates do not account for variability in the presence of gravel and also the soil structure. Within the plot scale, increasing plot size did not seem to have a strong impact on K_{eff} or reduce variability in K_{eff}. Especially for the shallow gravel formation at Barren Fork Creek, the plot scale (1 m × 1 m to 10 m × 10 m) appears to be within

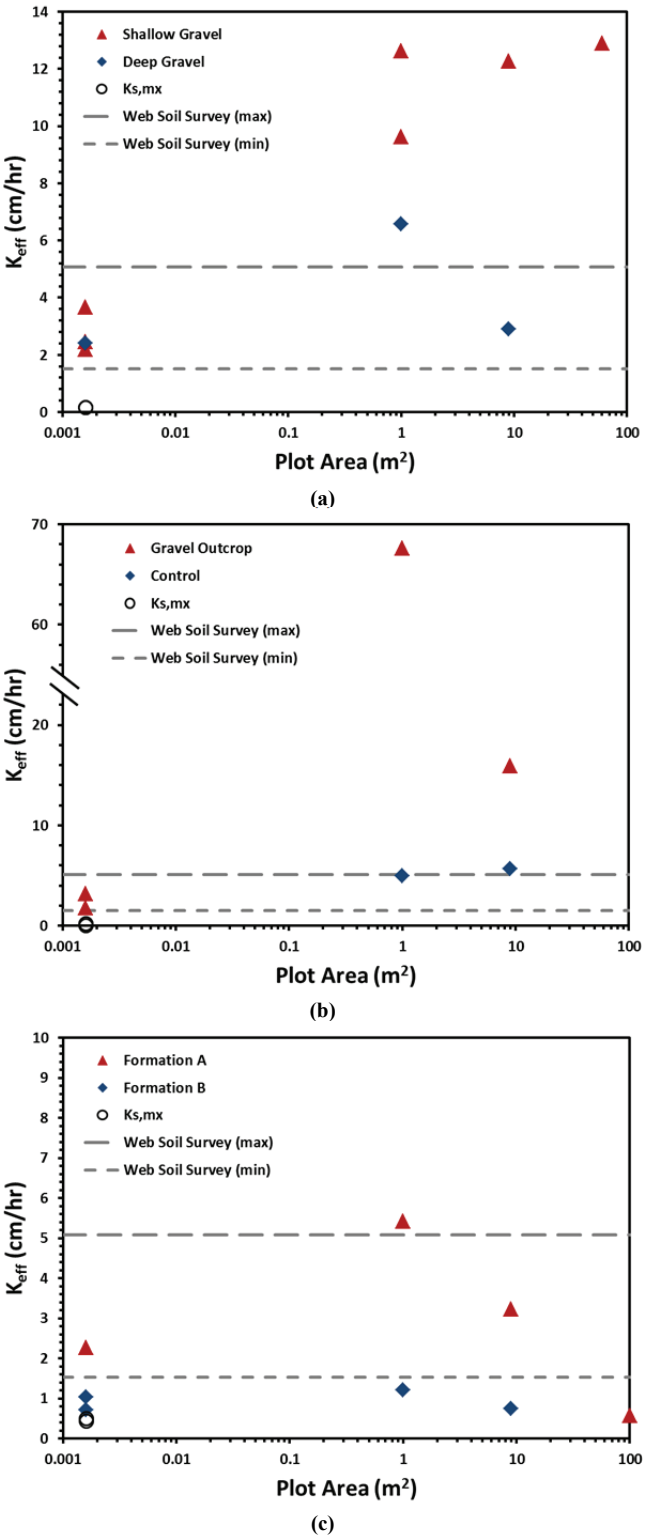

Figure 9. Effective saturated hydraulic conductivity (K_{eff}) data for the (a) Barren Fork Creek, (b) Pumpkin Hollow, and (c) Clear Creek floodplain sites, including both point-scale estimates and plot-scale infiltration experiments. The expected range of infiltration rates based on the permeability of the limiting layer reported in the USDA-NRCS Soil Survey (NRCS, 2012) is shown by the dashed lines. The matrix saturated hydraulic conductivity ($K_{s,mx}$) data were determined with a tension infiltrometer.

the REV. At the Pumpkin Hollow site, both point-scale data and NRCS soil survey data severely underestimated the capacity of the gravel outcrops to infiltrate water (fig. 9). This difference indicates the need for larger-scale field measurements of infiltration rate and K_{eff}. For example, soil survey measurements may represent a typical soil pedon but miss gravel outcrops or large macropores, which may be infrequent but have a disproportionate impact on infiltration. The agreement between the point-scale data and the NRCS estimates for both the Pumpkin Hollow and the Barren Fork Creek sites supports the idea that the NRCS data may be more representative of hydrological processes at a small scale rather than a plot or field scale. At the Clear Creek site, K_{eff} values from all three data sources were comparable (fig. 9). However, similar to the other sites, the point-scale estimates failed to capture the range in K_{eff} present in these floodplains. There was a negative correlation between K_{eff} and plot size at the Clear Creek site (similar to the gravel outcrop plots at the Pumpkin Hollow site). This could be due to the large variability in the data, making it difficult to discern the significance of the trend with limited data points. Additional infiltration plots would have enabled more rigorous statistics, but the effort required for plot-scale infiltration experiments made a large sample size prohibitive.

Impact of Macropores

Tension infiltrometers confirmed the importance of macropore flow. The $K_{s,mx}$ (in pore space less than or equal to 500 µm) was quantified with an infiltrometer tension of 6 cm and was one to two orders of magnitude lower than K_s (fig. 10). The $K_{s,mp}$ accounted for approximately 98% to 99% of the K_s at the Barren Fork Creek site, 84% to 86% at the Clear Creek site, and 97% to 99% at the Pumpkin Hollow site, indicating that even with macropores defined as greater than 500 µm instead of 75 µm, the vast majority of infiltration was occurring in macropores during the plot infiltration experiments. These data underscore the importance of fully accounting for the impact of macroporosity when determining hydraulic conductivity and modeling infiltration processes at a field scale (Ahuja et al., 2010).

Observed large macropores (greater than 1 cm) did not have as much impact on infiltration as expected. For example, a 4 to 5 cm diameter macropore was observed in the 10 m × 10 m plot at the Barren Fork Creek site. Subsequent excavation revealed that the macropore descended vertically to a depth of 1.0 m, into the gravel layer, before proceeding laterally 15 cm (fig. 11). Infiltration into this single macropore was quantified to be 27.4 L min^{-1} with head of 3.4 cm (the maximum ponded depth achieved during the plot-scale infiltration test) and up to 56.2 L min^{-1} with a head of 20 cm. However, a head of 0.4 cm, designed to better simulate natural rainfall conditions, resulted in a flow of only 1.3 L min^{-1}. As the diameter of a macropore increases, it has a larger capacity to transport water, but at some critical diameter this capacity surpasses typical rainfall rates and flow into the macropore becomes supply-limited. Macropores larger than this critical diameter do not have a larger actual flow rate and, assuming a typical soil pore size distribution, are less frequent. It is hypothesized that a dominant diameter, less than the critical diameter, is the pore size responsible for the most infiltration because it is large enough to have significant flow but small enough to

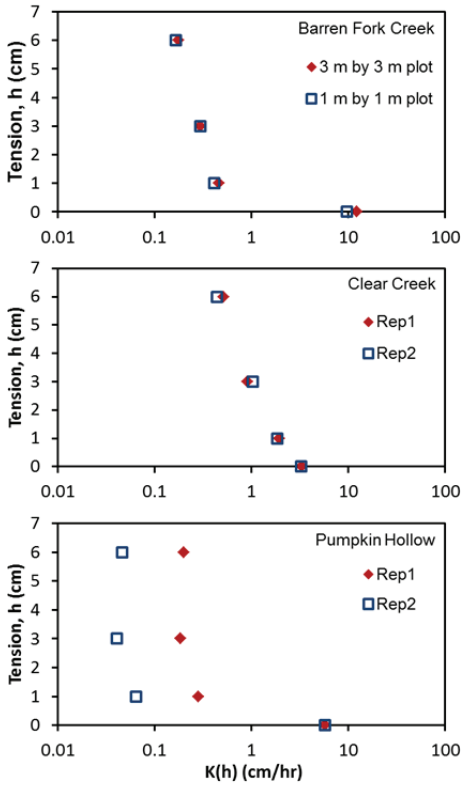

Figure 10. Hydraulic conductivity, $K(h)$, based on infiltration plots for saturated infiltration (h = 0 cm) and tension infiltrometer data for unsaturated infiltration (h > 0). Locations included shallow gravel plots at the Barren Fork Creek site, the 3 m × 3 m Formation A plot at the Clear Creek site, and the 3 m × 3 m control plot at the Pumpkin Hollow site.

Figure 11. (a) Large macropore at the Barren Fork Creek site observed during plot-scale infiltration experiment, and (b) subsequently filled with expandable foam and excavated.

occur frequently. In fact, this pore size range occurs frequently enough that it can be characterized sufficiently by 1 m × 1 m plots, explaining in part why they are included in the REV.

Research Implications

It was hypothesized that as the scale of measurement increases, the measured infiltration rate and calculated hydraulic conductivity of the topsoil will increase due to an increased likelihood of a very large but infrequent macropore occurring in a large plot size, and that the variability will decrease until an REV is attained (Bear, 1972; Brown et al., 2000). At all sites, the K_{eff} increased until the plot scale was reached (1 m × 1 m), but K_{eff} did not consistently increase or decrease as the plot scale increased from 1 m × 1 m to 10 m × 10 m. While variability in K_{eff} decreased as the scale increased from 1 m × 1 m to 3 m × 3 m at the Pumpkin Hollow and Clear Creek sites, the variability actually increased at the Barren Fork site as the scale of measurement increased from 1 m × 1 m to 3 m × 3 m. More specifically, the K_{eff} values were relatively constant within the plot scale for the shallow gravel formation (Barren Fork), the control plots (Pumpkin Hollow), and Formation B (Clear Creek). Therefore, it was concluded that the plot scale (1 to 100 m^2) is generally within the REV for geomorphic formations in these alluvial floodplains. Beyond the REV, the K_{eff} is expected to drift as different geomorphic formations are encountered.

In order to best characterize infiltration processes at the field scale, plot-scale infiltration tests are recommended over smaller-scale infiltrometer tests or point-scale estimates. In addition, since the 1 m × 1 m plot size is already within the REV, 1 m × 1 m plots are recommended. While a decrease in variability can be observed for larger plot sizes at the Pumpkin Hollow and Clear Creek sites, the level of difficulty in doing plot-scale infiltration measurements increases significantly at the 3 m × 3 m and especially the 10 m × 10 m scales. Instead of investing in larger plot sizes, more will be gained from investing in a higher number of 1 m × 1 m plots in order to accurately determine the mean K_{eff} for a field. Plots should ideally be randomly located and at least 27 m apart (based on A_0 for the Barren Fork site) in order to sample different geomorphic formations. In order to evaluate the number of plots necessary, the standard error of the mean was calculated according to Steel and Torrie (1980) for each floodplain site:

$$SE = \frac{s}{\sqrt{n}} \tag{4}$$

where SE is the standard error of the mean, s is the standard deviation, and n is the number of plots. The SE is a measure of how close a sample mean is to the population mean. While K_{eff} data tend to be more lognormally distributed, parametric statistics could be calculated with the small

Table 2. Statistics for effective saturated hydraulic conductivity (K_{eff}) derived from plot-scale infiltration experiments, including mean, standard deviation, and coefficient of variation, for each floodplain site. Hypothetical standard errors were calculated to evaluate the level of site characterization achieved for a range of sample sizes.

Statistic		Barren Fork Creek	Pumpkin Hollow	Clear Creek
Measured data				
n		6	4	5
Mean (cm h^{-1})		9.5	24	2.2
Standard deviation (cm h^{-1})		4.0	30	2.1
Coefficient of variation		0.4	1.3	0.9
		Standard Error of the Mean (cm h^{-1})		
Hypothetical *n*	1	4.0	30	2.1
	2	2.9	21	1.5
	3	2.3	17	1.2
	4	2.0	15	1.0
	5	1.8	13	0.9
	6	1.6	12	0.8

number of samples and give an indication of the level of site characterization achieved for a range of sample sizes (table 2).

For example, if three plot-scale infiltration experiments were performed at each site, the standard error of the mean would be 25% of the mean at the Barren Fork Creek site, 73% of the mean at the Pumpkin Hollow site, and 53% of the mean at the Clear Creek site. The Pumpkin Hollow site would be the most difficult to characterize with a low number of plots due to the high level of heterogeneity present. Future research should determine and compare the number of double ring infiltrometer measurements needed to the number of plot infiltration experiments needed to achieve an equivalent standard error of the mean for these field sites.

SUMMARY AND CONCLUSIONS

Effective saturated hydraulic conductivity (K_{eff}) data, based on plot-scale infiltration rates, were highly heterogeneous and reached 68 cm h^{-1} on one gravel outcrop. Point-scale estimates of K_{eff} were significantly lower than plot-scale K_{eff} and also failed to capture the variability of K_{eff} within a field site. The estimated permeability of the limiting layer reported by the USDA-NRCS Soil Survey was consistent with point-scale estimates of K_{eff} but was lower than plot-scale K_{eff} at most sites. For silt loam soils, infiltration was dominated by rapid macropore flow. Tension infiltrometers showed that macropores accounted for approximately 84% to 99% of the total saturated hydraulic conductivity, highlighting the difference between the conceptual infiltration model of a diffuse wetting front characterized by the Richards equation and actual infiltration in field conditions. The plot scale (1 to 100 m^2) generally appears to be within the representative elementary volume (REV), but drift in K_{eff} occurs beyond the REV due to changing geomorphic formations. Plot-scale infiltration tests are recommended over point-scale estimates, although only small plots (1 m × 1 m) are necessary. While this research does not definitively answer the question of scale impacts on infiltration, the results indicate that scale effects should be considered, as documented by the highly heterogeneous infiltration rates in these alluvial floodplains.

ACKNOWLEDGEMENTS

The project described in this article was supported by Grant/Cooperative Agreement No. G10AP00137 from the U.S. Geological Survey. Its contents are solely the responsibility of the authors and do not necessarily represent the official views of the USGS. This material was also developed under STAR Fellowship Assistance Agreement No. FP-917333 awarded by the U.S. Environmental Protection Agency (EPA). It has not been formally reviewed by EPA. The views expressed in this article are solely those of the authors, and EPA does not endorse any products or commercial services mentioned in this article.

The authors also acknowledge Mr. Dan Butler, Mrs. Shannon Robertson, Dr. Bill Huff, and Mrs. Sara Boelkins for providing access to their alluvial floodplain properties. David A. Correll, David T. Criswell, Dr. Todd Halihan, Devon Ketchum, Taber L. Midgley, Dr. Ronald B. Miller, Qualla J. Parman, and Peter Q. Storm of Oklahoma State University, and Jason Corral, Chad Walker, and Dr. Brian E. Haggard of the University of Arkansas, are acknowledged for their assistance with field and laboratory research. Dr. Ronald B. Miller, Qualla J. Parman, and Ryan P. Freiberger are acknowledged for their assistance with data analysis. Finally, a special thanks to Dr. Chad J. Penn for reviewing an earlier version of the manuscript.

REFERENCES

Ahuja, L. R., Ma, L., & Green, T. R. (2010). Effective soil properties of heterogeneous areas for modeling infiltration and redistribution. *SSSA J., 74*(5), 1469-1482. http://dx.doi.org/10.2136/sssaj2010.0073.

Akay, O., & Fox, G. A. (2007). Experimental investigation of direct connectivity between macropores and subsurface drains during infiltration. *SSSA J., 71*(5), 1600-1606. http://dx.doi.org/10.2136/sssaj2006.0359.

Bear, J. (1972). *Dynamics of Fluids in Porous Media.* New York, N.Y.: Elsevier.

Beven, K., & Germann, P. (1981). Water flow in soil macropores: 2. A combined flow model. *J. Soil Sci., 32*(1), 15-29. http://dx.doi.org/10.1111/j.1365-2389.1981.tb01682.x.

Beven, K., & Germann, P. (1982). Macropores and water flow in soils. *Water Resource Res., 18*(5), 1311-1325. http://dx.doi.org/10.1029/WR018i005p01311.

Biggar, J. W., & Nielsen, D. R. (1976). Spatial variability of the leaching characteristics of a field soil. *Water Resource Res., 12*(1), 78-84. http://dx.doi.org/10.1029/WR012i001p00078.

Bodhinayake, W., Si, B. C., & Noborio, K. (2004). Determination of hydraulic properties in sloping landscapes from tension and double-ring infiltrometers. *Vadose Zone J, 3*(3), 964-970. http://dx.doi.org/10.2136/vzj2004.0964.

Brown, G. O., Hsieh, H. T., & Lucero, D. A. (2000). Evaluation of laboratory dolomite core sample size using representative elementary volume concepts. *Water Resource Res., 36*(5), 1199-1207. http://dx.doi.org/10.1029/2000WR900017.

Bunte, K., & Abt, S. (2001). Sampling surface and subsurface particle-size distributions in wadable gravel and cobble bed streams for analyses in sediment transport, hydraulics, and streambed monitoring. USFS General Technical Report 74. Fort Collins, Colo.: USDA Rocky Mountain Research Station.

Carlyle, G. C., & Hill, A. R. (2001). Groundwater phosphate dynamics in a river riparian zone: Effects of hydrologic flowpaths, lithology, and redox chemistry. *J. Hydrol., 247*(3-4),

151-168. http://dx.doi.org/10.1016/S0022-1694(01)00375-4.
Djodjic, F., Katarina, B., & Bergstrom, L. (2004). Phosphorus leaching in relation to soil type and soil phosphorus content. *J. Environ. Qual., 33*(2), 678-684. http://dx.doi.org/10.2134/jeq2004.0678.
Easton, Z. M. (2013). Defining spatial heterogeneity of hillslope infiltration characteristics using geostatistics, error modeling, and autocorrelation analysis. *J. Irrig. Drain. Eng., 139*(9), 718-727. http://dx.doi.org/10.1061/(ASCE)IR.1943-4774.0000602.
Evans, R. G., Larue, J., Stone, K. C., & King, B. A. (2012). Adoption of site-specific variable-rate sprinkler irrigation systems. *Irrig. Sci., 31*(4), 871-887. http://dx.doi.org/10.1007/s00271-012-0365-x).
Fox, G. A., Malone, R. W., Sabbagh, G. J., & Rojas, K. (2004). Interrelationship of macropores and subsurface drainage for conservative tracer and pesticide transport. *J. Environ. Qual., 33*(6), 2281-2289. http://dx.doi.org/10.2134/jeq2004.2281.
Fox, G. A., Heeren, D. M., Miller, R. B., Mittelstet, A. R., & Storm, D. E. (2011). Flow and transport experiments for a streambank seep originating from a preferential flow pathway. *J. Hydrol.,* 403(3-4), 360-366, 10.1016/j.jhydrol.2011.04.014.
Fuchs, J. W., Fox, G. A., Storm, D. E., Penn, C. J., & Brown, G. O. (2009). Subsurface transport of phosphorus in riparian floodplains: Influence of preferential flow paths. *J. Environ. Qual., 38*(2), 473-484. http://dx.doi.org/10.2134/jeq2008.0201.
Gburek, W. J., Barberis, E., Haygarth, P. M., Kronvang, B., & Stamm, C. (2005). Chapter 29: Phosphorus mobility in the landscape. In J. Sims, & A. N. Sharpley (Eds.), *Phosphorus: Agriculture and the Environment* (pp. 941-979). Madison, Wisc.: ASA-CSSA-SSSA.
Gold, A. J., & Kellogg, D. (1997). Modelling internal processes of riparian buffer zones. In N. Haycock (Ed.), *Buffer Zones: Their Processes and Potential in Water Protection* (pp. 192-207). Harpenden, U.K.: Quest Environmental.
Gotovac, H., Cvetkovic, V., & Andricevic, R. (2009). Flow and travel time statistics in highly heterogeneous porous media. *Water Resources Res., 45*(7), W07402. http://dx.doi.org/10.1029/2008WR007168.
Halihan, T., Paxton, S., Graham, I., Fenstemaker, T., & Riley, M. (2005). Post-remediation evaluation of a LNAPL site using electrical resistivity imaging. *J. Environ. Monit., 7*(4), 283-287. http://dx.doi.org/10.1039/b416484a.
Heeren, D. M. (2012). Subsurface phosphorus transport and scale-dependent phosphorus leaching in alluvial flood-plains. PhD diss. Stillwater, Okla.: Oklahoma State University, Department of Biosystems and Agricultural Engineering.
Heeren, D. M., Miller, R. B., Fox, G. A., Storm, D. E., Penn, C. J., & Halihan, T. (2010). Preferential flow path effects on subsurface contaminant transport in alluvial floodplains. *Trans. ASABE, 53*(1), 127-136. http://dx.doi.org/10.13031/2013.29511.
Heeren, D. M., Fox, G. A., Miller, R. B., Storm, D. E., Mittelstet, A. R., Fox, A. K., Penn, C. J., & Halihan, T. (2011). Stage-dependent transient storage of phosphorus in alluvial floodplains. *Hydrol. Proc., 25*(20), 3230-3243. http://dx.doi.org/10.1002/hyp.8054.
Heeren, D. M., Fox, G. A., & Storm, D. E. (2014a). Technical note: Berm method for quantification of infiltration at the plot scale in high conductivity soils. *J. Hydrol. Eng., 19*(2), 457-461. http://dx.doi.org/10.1061/(ASCE)HE.1943-5584.0000802.
Heeren, D. M., Fox, G. A., Fox, A. K., Storm, D. E., Miller, R. B., & Mittelstet, A. R. (2014b). Divergence and flow direction as indicators of subsurface heterogeneity and stage-dependent storage in alluvial floodplains. *Hydrol. Proc., 28*(3), 1307-1317. http://dx.doi.org/10.1002/hyp.9674.
Lai, J., & Ren, L. (2007). Assessing the size dependency of measured hydraulic conductivity using double-ring infiltrometers and numerical simulation. *SSSA J., 71*(6), 1667-1675. http://dx.doi.org/10.2136/sssaj2006.0227.
Massman, J. W. (2003). Implementation of infiltration ponds research. Final research report. Olympia, Wash.: Washington State Transportation Commission.
Midgley, T. L., Fox, G. A., & Heeren, D. M. (2012). Evaluation of the Bank Stability and Toe Erosion Model (BSTEM) for predicting lateral streambank retreat on composite streambanks. *Geomorphology, 145-146*, 107-114. http://dx.doi.org/10.1016/j.geomorph.2011.12.044.
Miller, R. B. (2012). Hydrogeophysics of gravel-dominated alluvial floodplains in eastern Oklahoma. PhD diss. Stillwater, Okla.: Oklahoma State University, Department of Biosystems and Agricultural Engineering.
Miller, R. B., Heeren, D. M., Fox, G. A., Storm, D. E., & Halihan, T. (2011). Design and application of a direct-push vadose zone gravel permeameter. *Ground Water, 49*(6), 920-925. http://dx.doi.org/10.1111/j.1745-6584.2010.00796.x.
Miller, R. B., Heeren, D. M., Fox, G. A., Halihan, T., Storm, D. E., & Mittelstet, A. R. (2014). The hydraulic conductivity structure of gravel-dominated vadose zones within alluvial floodplains. *J. Hydrol., 513*, 229-240. http://dx.doi.org/10.1016/j.jhydrol.2014.03.046.
Mulholland, P. J., Wilson, G. V., & Jardine, P. M. (1990). Hydrogeochemical response of a forested watershed to storms: Effects of preferential flow along shallow and deep pathways. *Water Resources Res., 26*(12), 3021-3036. http://dx.doi.org/10.1029/WR026i012p03021.
Najm, M. R., Jabro, J. D., Iverson, W. M., Mohtar, R. H., & Evans, R. G. (2010). New method for the characterization of three-dimensional preferential flow paths in the field. *Water Resources Res., 46*(2), W02503. http://dx.doi.org/10.1029/2009WR008594.
Nelson, N. O., Parsons, J. E., & Mikkelson, R. L. (2005). Field-scale evaluation of phosphorus leaching in acid sandy soils receiving swine waste. *J. Environ. Qual., 34*(6), 2024-2035. 10.2134/jeq2004.0445. http://dx.doi.org/10.2134/jeq2004.0445.
NRCS. (2012). Web Soil Survey (WSS). Washington, D.C.: USDA Natural Resources Conservation Service. Retrieved from http://websoilsurvey.nrcs.usda.gov/.
Philip, J. R. (1957). The theory of infiltration: 1. The infiltration equation and its solution. *Soil Sci., 83*(5), 345-358. http://dx.doi.org/10.1097/00010694-195705000-00002.
Polyakov, V., Fares, A., & Ryder, M. H. (2005). Precision riparian buffers for the control of nonpoint-source pollutant loading into surface water: A review. *Environ. Reviews, 13*(3), 129-144. http://dx.doi.org/10.1139/a05-010.
Sauer, T. J., & Logsdon, S. D. (2002). Hydraulic and physical properties of stony soils in a small watershed. *SSSA J., 66*(6), 1947-1956. http://dx.doi.org/10.2136/sssaj2002.1947.
Sauer, T. J., Logsdon, S. D., Van Brahana, J., & Murdoch, J. F. (2005). Variation in infiltration with landscape position: Implications for forest productivity and surface water quality. *Forest Ecol. Mgmt., 220*(1-3), 118-127. http://dx.doi.org/10.1016/j.foreco.2005.08.009.
Scott, H. D. (2000). *Soil Physics: Agricultural and Environmental Applications.* Ames, Iowa: Iowa State University Press.
Simunek, J., Jarvis, N. J., van Genuchten, M. T., & Gardenas, A. (2003). Review and comparison of models for describing non-equilibrium and preferential flow and transport in the vadose zone. *J. Hydrol., 272*(1-4), 14-35. http://dx.doi.org/10.1016/S0022-1694(02)00252-4.
Sisson, J. B., and P. J. Wierenga. 1981. Spatial variability of steady-state infiltration rates as a stochastic process. *SSSA J., 45*(4), 699-704.
SSSA. (2008). Glossary of soil science terms. Madison, Wisc.:

SSSA. Retrieved from https://www.soils.org/publications/soils-glossary.
Steel, R. G. D., & Torrie, J. H. (1980). *Principles and Procedures of Statistics.* New York, N.Y.: McGraw-Hill.
Thomas, G. W., & Phillips, R. E. (1979). Consequences of water movement in macropores. *J. Environ. Qual., 8*(2), 149-152. http://dx.doi.org/10.2134/jeq1979.00472425000800020002x.
USEPA. (2009). Pathogen TMDLs for Clear Creek 11110103-029 in Arkansas Planning Segment 3J. Dallas, Tex.: U.S. EPA Region 6, Water Quality Protection Division.
van Genuchten, M. T., Leij, F. J., & Yates, S. R. (1991). The RETC code for quantifying the hydraulic functions of unsaturated soils. EPA/600/2-91/065. Riverside, Cal.: USDA-ARS U.S. Salinity Laboratory.
Vellidis, G., Lowrance, R., Hubbard, R., & Gay, P. (2001). Preferential flow caused by past disturbance in a restored riparian wetland. In D. D. Bosch, & K. King (Ed.), *Proc. 2nd Intl. Symp. Preferential Flow: Water Movement and Chemical Transport in the Environment*, (pp. 61-64). St. Joseph, Mich.: ASAE.
Vieira, S. R., Nielsen, D. R., & Biggar, J. W. (1981). Spatial variability of field-measured infiltration rate. *SSSA J., 45*(6), 1040-1048. http://dx.doi.org/10.2136/sssaj1981.03615995004500060007x.
Zhang, R. (1997). Determination of soil sorptivity and hydraulic conductivity from the disk infiltrometer. *SSSA J., 61*(4), 1024-1030. http://dx.doi.org/10.2136/sssaj1997.03615995006100040005x.